

Direct observation of the soft mode in the paraelectric phase of PbTiO_3 by confocal micro-Raman scattering

Hwee Ping Soon, Hiroki Taniguchi, Yasuhiro Fujii, and Mitsuru Itoh*
Materials and Structures Laboratory, Tokyo Institute of Technology, Yokohama 226-8503, Japan

Makoto Tachibana
National Institute for Materials Science, Tsukuba 305-0044, Japan

(Received 30 August 2008; revised manuscript received 17 October 2008; published 12 November 2008)

The soft mode behavior in PbTiO_3 (PT) single crystal has been revisited by our confocal micro-Raman measurements. Contrary to the common understandings, the temperature dependence of soft mode in the cubic PT paraelectric phase was precisely resolved for the first time, owing to the existence of macroscopic size Raman active regions (≥ 780 nm). By evidently ruling out the possibility of defect-induced Raman scattering, the elasto-optical coupling serves as the most likely mechanism for the occurrence of these Raman active regions.

DOI: 10.1103/PhysRevB.78.172103

PACS number(s): 77.80.Bh, 63.20.-e, 77.84.-s, 78.30.-j

The ferroelectric ABO_3 perovskite oxides have been constantly drawing numerous interests in many aspects since the last few decades. Among all the ABO_3 perovskites, PbTiO_3 (PT) plays an extremely important role, whereby the progressive research activities have led to tremendous advancement in both the fundamental understandings in structural phase transition and the innovations of modern devices. In terms of technological considerations, PT serves as the essential parent material for many high-performance piezoelectric solid solutions, such as for the well-known $\text{Pb}(\text{Zr}_{1-x}\text{Ti}_x)\text{O}_3$ (PZT), $(1-x)\text{PbTiO}_3-x\text{Pb}(\text{Mg}_{1/3}\text{Nb}_{2/3})\text{O}_3$ (PMN-PT), and $(1-x)\text{PbTiO}_3-x\text{Pb}(\text{Zn}_{1/3}\text{Nb}_{2/3})\text{O}_3$ (PZN-PT) that have been employed in many commercial applications.¹ In addition to the technological importance, PT also acts as a long-standing textbook example for the displacive-type phase transition, as confirmed by many in-depth experimental²⁻⁹ and theoretical¹⁰⁻¹³ investigations. These studies unambiguously suggested that the phase transition of PT is brought about by the softening of the lowest-frequency transverse optical (TO) modes.

Despite PT has been subjected to many rigorous studies, a precise experimental data on the soft mode behavior for its cubic paraelectric phase still remains unavailable. Numerous efforts have been devoted to such issue by inelastic neutron scattering,^{3,6} infrared,¹⁴ and Raman scattering techniques;^{7,8} however, the difficulty in synthesizing a high-quality large single crystal has retarded the direct observation.¹⁵ Although the inelastic neutron-scattering measurements reported by Shirane *et al.*³ indicated that the softening of soft mode with decreasing temperature (T) in PT paraelectric phase obeys the Curie-Weiss law with $T_0 \sim 449$ °C, which is qualitatively in agreement with that obtained from the dielectric measurements,¹⁶ the T dependence of the soft mode energy at $q=0$ was approximately deduced by extrapolating the energy measured from $q=0.08$ to 0.2 for each T . Indeed, direct observation on the soft mode in PT paraelectric phase at $q=0$ failed due to the presence of broad neutron group and strong acoustic phonons at elevated T . Recently, Kempa *et al.*⁶ reinvestigated the phonon-dispersion curves for PT paraelectric phase using the same technique. In contrast to

the report by Shirane *et al.*,³ direct observation on the soft TO branch at $q=0$ has been achieved at $T_c + 15 \leq T \leq T_c + 290$ °C, whereby the soft mode was found to soften down to 44.4 cm^{-1} ; however, no data was available in the vicinity of T_c although it contains physically important information about the phase transition. Also, the access of soft mode behavior by infrared technique failed due to the ill-defined infrared peak in PT paraelectric phase. To surmount the difficulty in obtaining high-quality large single crystal, Fontana *et al.*^{7,8} again investigated the spectrum for PT paraelectric phase using Raman scattering technique; however, no soft mode was resolved. On the other hand, the soft mode observed by Raman scattering technique in the centrosymmetric $\text{SrTi}^{18}\text{O}_3$ (Refs. 17 and 18) and KTaO_3 (Ref. 19) paraelectric phase due to the local symmetry breaking has indeed shed light on the possibility for resolving the soft mode in PT paraelectric phase. In this Brief Report, we report the precise observation on the soft mode in PT paraelectric phase at $T_c (= 496$ °C) $\leq T \leq 600$ °C using a confocal micro-Raman system. The confocal micro-Raman technique allows us to select the optically homogenous region, whereby the intensity that did not originate from the selected scattered volume is effectively attenuated. The employment of long accumulation time, therefore, enables the improvement of the signal to noise ratio.

The confocal micro-Raman measurements were performed by the Jobin-Yvon T64000 with triple monochromator micro-Raman system with the aids of a high objective lens (N.A.=0.5) and a 514.5-nm Ar^+ green laser (~ 10 mW). A transparent nonconductive PT single crystal ($1 \times 1 \times 0.3$ mm^3) with (001) surface that was polished up to the optical quality was employed. Prior to the measurement, a single domain region was carefully determined by ensuring the same angular and positional dependence of Raman spectra. The laser with a spot size of ~ 1 μm was focused onto the selected area ~ 15 μm below the sample surface. The polarized scattered light was collected by a back scattering geometry $Z(X, Y)\bar{Z}$, where X , Y , and Z correspond to sample coordinates $[100]$, $[010]$, and $[001]$ of the cubic paraelectric phase, respectively. Furthermore, Raman spectra at various T

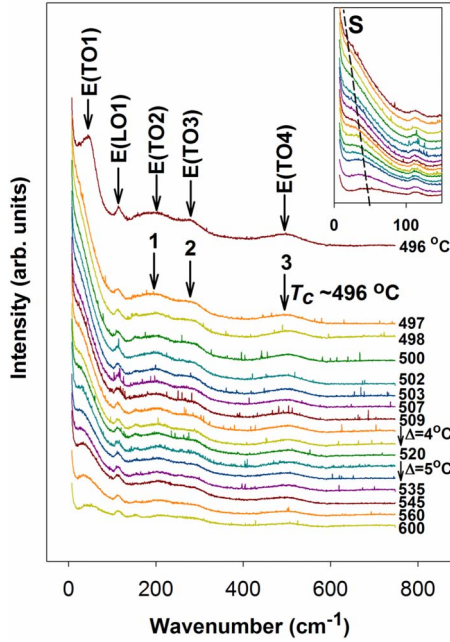


FIG. 1. (Color online) Raman spectra of PT measured at $T_c = 496 \leq T \leq 600$ °C upon heating, where Δ denotes the T interval involved in the heating process. The spectrum obtained at 496 °C corresponds to the spectrum of PT ferroelectric phase. The inset shows the hardening of mode S for PT paraelectric phase with increasing T .

were obtained by employing a heating stage Linkam TS1500 with T stability of ± 1 °C.

Figure 1 depicts the Raman spectra of PT measured at $496 \leq T \leq 600$ °C. Agreeing with the previous report, the Raman modes at ~ 46 , 190, 280, and 493 cm^{-1} observed in the spectrum at 496 °C correspond to the E(TO1), E(TO2), E(TO3), and E(TO4) of PT ferroelectric phase, respectively, where E(TO1), E(TO2), and E(TO4) originated from the T_{1u} modes, whereas E(TO3) is from the T_{2u} silent mode of the cubic paraelectric phase.^{2,8} In addition to the four E(TO) modes, there occurs a relatively weak mode at ~ 120 cm^{-1} that is forbidden by the Raman selection rules. Apparently, the E(LO1) “leakage” brought about by the contribution from the nonaxial rays of light that are inevitable with the usage of high N. A. lens in our system serves as the most possible factor for the occurrence of this mode.²⁰ Similar mode was also observed by Foster *et al.*²¹ in their high-resolution Raman measurement for PT with the same scattering geometry.

Upon heating, the soft E(TO1) mode in the ferroelectric phase suddenly vanishes at 497 °C and a central-peak (CP)-like spectrum is then observed for the PT paraelectric phase. Such a CP-like spectrum persists with some gradual changes at $497 \leq T \leq 503$ °C. Further heating results in the appearance of a Raman mode together with the CP-like spectrum. Interestingly, it is found that the frequency of this Raman mode (mode S) hardens with increasing T , as shown in the inset of Fig. 1. In contrast to mode S , modes 1 to 3 in PT paraelectric phase exhibit no abrupt change in frequency but become broad and decrease in intensity with increasing T . The key question now is the origin of these modes in the PT

paraelectric phase. First, we analyze mode S , the soft-mode-like feature, by assuming the occurrence of defect-induced Raman scattering (DIRS) with the model proposed by Uwe *et al.*,¹⁹ whereby the scattering intensity $I_s(\omega)$ for mode S is described by

$$I_s(\omega) = \int W(q) I'(q, \omega) dq, \quad (1)$$

with

$$W(q) \propto \frac{1}{1 + q^2 R^2},$$

and

$$I'(q, \omega) \propto \frac{\omega_q^2 \omega \Gamma_s}{(\omega_q^2 - \omega^2)^2 + (\omega \Gamma_s)^2}.$$

R and Γ_s are the sizes of the Raman active region normalized by lattice parameter a and damping constant, respectively. $\omega_q = (\omega_{so}^2 + D^2 q^2)^{0.5}$ is the soft-mode frequency at wave number q . By referring to the previous studies, the lattice parameter a and phonon dispersion D are 3.915 Å and 1900 $\text{meV} \text{Å}$, respectively.^{6,16} Moreover, two assumptions were employed when performing the fittings with this model. First, the spectrum ranging from 131 to 602 cm^{-1} was assumed to have negligible influence on the low-frequency spectrum, whereby it was masked from the fitting. Second, the mode at ~ 120 cm^{-1} is considered as a constant background, which is described by a damped harmonic oscillator (DHO) that superimposes onto the low-frequency spectrum. The overall scattering intensity $I(\omega)$ with this model is, therefore,

$$I(\omega) \propto \left[\frac{n(\omega) + 1}{n(\omega)} \right] \left[\frac{S_r \omega \tau}{1 + (\omega \tau)^2} + S_s I_s + \frac{S_{bo} \omega_{bo}^2 \omega \Gamma_b}{(\omega_{bo}^2 - \omega^2)^2 + (\omega \Gamma_b)^2} \right]. \quad (2)$$

The $n(\omega)$ term in the first bracket denotes the population factor, while the three terms in the second bracket correspond to the CP, mode S , and the mode at ~ 120 cm^{-1} , where S_r , S_s , and S_{bo} are the amplitudes associated with CP, mode S , and the mode at 120 cm^{-1} , and τ , ω_{bo} , and Γ_b are relaxation time of the CP, harmonic frequency, and the damping constant for the mode at 120 cm^{-1} , respectively. Figure 2(a) plots the fitting of the spectrum observed at 520 °C to Eq. (2) with $R=2, 6$, and 2000, respectively. It is important to note that the fitted parameters $\omega_{so}=66.6$ cm^{-1} , $\Gamma_s=95.5$ cm^{-1} , and $\tau=6.11 \times 10^{-11}$ s remain the same for these three cases. Obviously, good fitting can only be obtained with large $R=2000$, indicating that the first-order Raman scattering resulted from rather large-size Raman active regions. Interestingly, this implies that the Raman scattering observed in PT paraelectric phase did not originate from ferroelectric microregions (FMR) induced by the symmetry-breaking point defects, such as vacancies or impurities, that encompass only dozens of unit cells (e.g., $R \sim 50$).¹⁹ Furthermore, we observed negligible change in fitting at $R > 2000$

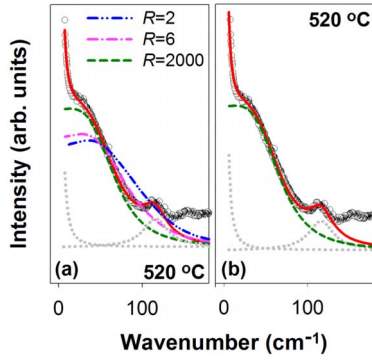


FIG. 2. (Color online) The fittings of Raman spectrum obtained for PT paraelectric phase at 520 °C (solid lines) by employing the DIRS with $R=2000$ (a) and the normal DHO (b) models, respectively. The dashed lines show the fitting results for mode S , while the dotted lines indicate the fittings to the CP and the forbidden mode at ~ 120 cm^{-1} that is considered as a constant background. The broad spectra indicated by the dash-double-dotted and the dash-dotted lines in (a) are the best fittings for mode S to the DIRS model with $R=2$ and 6, respectively.

when other parameters are kept constant, indicating that the size of Raman active regions (≥ 780 nm) is at least larger than the wavelength of the incident light.

Since the analyses by DIRS model suggested that the spectra observed for PT paraelectric phase resulted from rather large size Raman active regions, we again analyze the low-frequency spectra by a normal DHO model without considering the scattering intensity associated with the defects induced density of states, as described by Eq. (1). In this model, I_s in Eq. (2) is replaced by

$$I_s(\omega) = \frac{\omega_{so}^2 \omega \Gamma_s}{(\omega_{so}^2 - \omega^2)^2 + (\omega \Gamma_s)^2}, \quad (3)$$

where ω_{so} and Γ_s are the harmonic frequency and damping constant for mode S , respectively. Figure 2 shows an example of fitting to the Raman spectrum obtained at 520 °C to the normal DHO model. Equally good fitting was obtained with the same parameters ω_{so} , Γ_s , and τ suggested by the previous DIRS model with $R=2000$. The real frequency ω_s for mode S observed in PT paraelectric phase is further determined by $\omega_s = [\omega_{so}^2 - (\Gamma_s/2)^2]^{1/2}$, which corresponds to the frequency that coincides with the intervals between the times when the amplitude becomes zero for a DHO. The T dependence for ω_{so} , half width half maximum ($\text{HWHM} = \Gamma_s/2$), and ω_s , respectively, are further shown in Figs. 3(a) and 3(b). Now we verify these results by the comparisons with previous studies. First, as shown in Fig. 3(a), the frequency of ω_{so} increases whereas the HWHM decreases with increasing T , where the frequency for ω_{so} is always greater than HWHM, indicating that mode S for PT paraelectric phase is completely underdamped within the whole T range. This observation indeed pointed out that mode S is the soft mode in PT paraelectric phase on the basis of the consistency with the previous observation of underdamped soft mode at much higher T by the inelastic neutron-scattering technique.^{3,6} Second, the squared frequency of mode S observed in PT

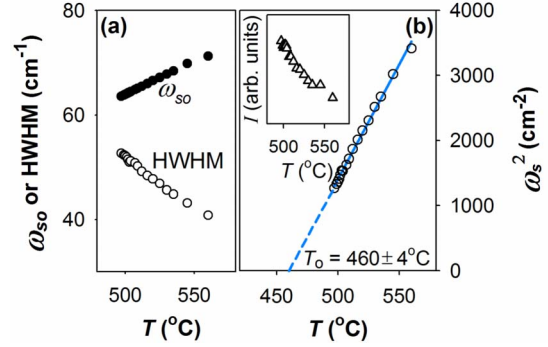


FIG. 3. (Color online) T dependences of ω_{so} and HWHM (a), and ω_s of soft mode (b), respectively, where the solid line shows the fitting to the Cochran's theory with an extrapolated $T_0 = 460 \pm 4$ °C. The inset in (b) demonstrates the T dependence of the fitted intensity for mode S .

paraelectric phase, ω_s^2 increases linearly with increasing T , whereby the linear fitting to the Cochran's theory,²² $\omega_s^2 = A(T - T_0)$, gives $A = 35.3$ and $T_0 = 460 \pm 4$ °C, respectively. This extrapolated T_0 is comparable to those suggested by the inelastic neutron scattering and dielectric measurements for PT,^{3,9} which further confirms that mode S is the soft mode in PT paraelectric phase. Third, in comparison to the soft mode frequency at 44.4 cm^{-1} obtained by inelastic neutron scattering at $T = T_c + 15$ °C,⁶ which is currently the lowest attainable T for a direct observation of soft mode at $q=0$, we obtained 42.3 cm^{-1} for mode S at the same T , again showing a good consistency with the previous measurement. On the basis of these three strong agreements with the previous reports, we can unambiguously confirm that mode S is the soft mode in PT paraelectric phase, which has indeed been plausibly resolved for the first time down to the vicinity of T_c , whereby a discontinuity at 35.6 cm^{-1} at $T_c + 1$ °C was obtained. Also, these agreements confirm that the local heating problem is negligible in our measurement. Similar to mode S , the soft mode in paraelectric phase, modes 1 and 3 can be apparently assigned as the T_{1u} modes, while mode 2 as the T_{2u} mode. Since the phase transition from cubic to tetragonal result in four E modes in the same frequencies as those of cubic T_{1u} and T_{2u} modes,²¹ the frequencies of modes 1 to 3 that are similar to those of E(TO) modes in the ferroelectric phase support these assignments. However, the occurrence of silent T_{2u} in the spectra is currently unknown and pending for further investigations.

Now we discuss the possible origin for the existence of large-size Raman active regions in PT paraelectric phase. When the cubic polar modes are vibrating, the polarization fluctuations (ΔP) are induced accordingly. Due to the presence of electrostrictive coupling in all dielectric materials and even in their paraelectric phases, such fluctuations are accompanied by the occurrence of local strain e_{lm} that can be described by

$$-\frac{\Delta \varepsilon_{ij}}{\varepsilon_0} \equiv \sum_{l,m} p_{ijlm} e_{lm}, \quad (4)$$

where the coefficients p_{ijlm} are the elasto-optical constants.²³ It is well known that $I(\omega)$ is proportional to $\langle \Delta \varepsilon_{ij}^2 \rangle$ in the

range of optical frequency.²⁴ Therefore, the occurrence of ΔP induces $\Delta\epsilon_{ij}$ so as the $I(\omega)$.²⁵ Since the vibration amplitude of soft mode is larger than other cubic polar modes, higher $I(\omega)$ is then induced, as shown in Fig. 1. This is particular so when the amplitude of soft mode so as ΔP becomes large near T_c , as evidenced by the increasing $I(\omega)$ with decreasing T shown in the inset of Fig. 3(b). However, $I(\omega)$ resulted from such mechanism is rather small compared to the usual Raman scattering processes. Therefore, such a small and material-dependent signal has not always been observed or neglected as noise. In contrast, our rigorous high-gain measurements have surmounted the difficulty in resolving the small signal from elastic-optical coupling, leading to the successful observation of soft mode in PT paraelectric phase, which further agrees with the studies that show the importance contribution of ΔP and strain coupling to strong first-order nature of PT phase transition.^{12,26}

In conclusion, the soft mode in PT paraelectric phase has been precisely resolved by our confocal micro-Raman measurements from T_c to 600 °C, whereby the drawbacks due to

the requirement of large single crystal have been overcome. This direct observation of soft mode evidently opposes the conventional belief that there occurs no first-order Raman scattering in the centrosymmetric PT paraelectric phase. Also, it is discovered that the first-order Raman spectra originated from the macroscopic-size Raman active regions in paraelectric phase, which is in contrast to the FMR induced by symmetric breaking defects. Our direct observation of soft mode in PT paraelectric phase strongly urges the immediate explorations on the Raman scattering in centrosymmetric phase with both theoretical and experimental approaches, which have been neglected previously. Again, new advancement has been triggered in the scientifically and technologically important PT.

This work was supported by both KAKENHI (Grant No. 20248098) and Global COE program, Education and Research Center for Material Innovation-Program for Upbringing International Leaders on Future Materials.

*itoh.m.aa@m.titech.ac.jp

¹K. Uchino, *Ferroelectric Devices* (Dekker, New York, 2000), Chap. 7, p. 145.

²G. Burns and B. A. Scott, *Phys. Rev. Lett.* **25**, 167 (1970).

³G. Shirane, J. D. Axe, and J. Harada, *Phys. Rev. B* **2**, 155 (1970).

⁴J. Hlinka, M. Kempa, J. Kulda, P. Bourges, A. Kania, and J. Petzelt, *Phys. Rev. B* **73**, 140101 (2006).

⁵I. Tomeno, Y. Ishii, Y. Tsunoda, and K. Oka, *Phys. Rev. B* **73**, 064116 (2006).

⁶M. Kempa, J. Hlinka, J. Kulda, P. Bourges, A. Kania, and J. Petzelt, *Phase Transitions* **79**, 351 (2006).

⁷M. D. Fontana, H. Idrissi, and K. Wojcik, *Europhys. Lett.* **11**, 419 (1990).

⁸M. D. Fontana, H. Idrissi, G. E. Kugel, and K. Wojcik, *J. Phys.: Condens. Matter* **3**, 8695 (1991).

⁹M. E. Lines and A. M. Glass, *Principles and Applications of Ferroelectrics and Related Materials* (Clarendon, Oxford, 1977), Chap. 8, p. 248.

¹⁰W. Zhong, R. D. King-Smith, and D. Vanderbilt, *Phys. Rev. Lett.* **72**, 3618 (1994).

¹¹A. Garcia and D. Vanderbilt, *Phys. Rev. B* **54**, 3817 (1996).

¹²U. V. Waghmare and K. M. Rabe, *Phys. Rev. B* **55**, 6161 (1997).

¹³R. E. Cohen, *Nature (London)* **358**, 136 (1992).

¹⁴N. E. Tornberg and C. H. Perry, *J. Chem. Phys.* **53**, 2946 (1970).

¹⁵M. C. Gelabert, R. A. Laudise, and R. E. Riman, *J. Cryst. Growth* **197**, 195 (1999).

¹⁶G. Shirane and S. Hoshino, *J. Phys. Soc. Jpn.* **6**, 265 (1951).

¹⁷H. Taniguchi, M. Itoh, and T. Yagi, *Phys. Rev. Lett.* **99**, 017602 (2007).

¹⁸M. Takesada, M. Itoh, and T. Yagi, *Phys. Rev. Lett.* **96**, 227602 (2006).

¹⁹H. Uwe, K. B. Lyons, H. L. Carter, and P. A. Fleury, *Phys. Rev. B* **33**, 6436 (1986).

²⁰K. J. Baldwin, D. N. Batchelder, and S. Webster, in *Handbook of Raman Spectroscopy from the Research Laboratory to the Process Lines*, edited by I. R. Lewis and H. G. M. Edwards, 1st ed. (Dekker, New York, 2001), Chap. 4, p. 145.

²¹C. M. Foster, Z. Li, M. Grimsditch, S.-K. Chan, and D. J. Lam, *Phys. Rev. B* **48**, 10160 (1993).

²²W. Cochran, *Adv. Phys.* **9**, 387 (1960).

²³G. B. Benedek and K. Fritish, *Phys. Rev.* **149**, 647 (1966).

²⁴R. W. Boyd, *Nonlinear Optics*, 2nd ed. (Academic, New York, 2003), Vol. 1, Chap. 8, p. 383.

²⁵A. P. Levanyuk, *Sov. Phys. JETP* **43**, 652 (1976).

²⁶G. Shirane, *Rev. Mod. Phys.* **46**, 437 (1974).